



OPEN ACCESS

EDITED BY

Sarika Gunjan,
Medical College of Wisconsin, United States

REVIEWED BY

Carla Claser,
Federal University of São Paulo, Brazil
Zeynep Islek,
Yeditepe University, Türkiye

*CORRESPONDENCE

Flávia Lima Ribeiro-Gomes
✉ flavia.gomes@ioc.fiocruz.br

RECEIVED 10 September 2024

ACCEPTED 08 July 2025

PUBLISHED 23 July 2025

CITATION

Freire-Antunes L, Ornellas-Garcia U,
Rangel-Ferreira M, Ribeiro-Almeida ML,
Carvalho LJM, Daniel-Ribeiro CT and
Ribeiro-Gomes FL (2025) Microglia exhibit a
dynamic response, modulating inducible
nitric oxide synthase expression and the
production of pro-inflammatory cytokines
during experimental cerebral malaria.
Front. Immunol. 16:1494418.
doi: 10.3389/fimmu.2025.1494418

COPYRIGHT

© 2025 Freire-Antunes, Ornellas-Garcia,
Rangel-Ferreira, Ribeiro-Almeida, Carvalho,
Daniel-Ribeiro and Ribeiro-Gomes. This is an
open-access article distributed under the terms
of the [Creative Commons Attribution License](#)
(CC BY). The use, distribution or reproduction
in other forums is permitted, provided the
original author(s) and the copyright owner(s)
are credited and that the original publication
in this journal is cited, in accordance with
accepted academic practice. No use,
distribution or reproduction is permitted
which does not comply with these terms.

Microglia exhibit a dynamic response, modulating inducible nitric oxide synthase expression and the production of pro-inflammatory cytokines during experimental cerebral malaria

Lucas Freire-Antunes, Uyla Ornellas-Garcia,
Marcos Rangel-Ferreira, Mônica Lucas Ribeiro-Almeida,
Leonardo José Moura Carvalho, Cláudio Tadeu Daniel-Ribeiro
and Flávia Lima Ribeiro-Gomes*

Laboratório de Pesquisa em Malária, Instituto Oswaldo Cruz and Centro de Pesquisa, Diagnóstico e Treinamento em Malária (CPD-Mal) of Fundação Oswaldo Cruz (Fiocruz) and of Secretaria de Vigilância em Saúde (SVS), Ministério da Saúde, Rio de Janeiro, Brazil

Microglia play a fundamental role in maintaining central nervous system homeostasis by monitoring brain tissue for physical, structural, and biochemical alterations. Its involvement in the pathogenesis of various neurological disorders is well documented. However, the role of microglia in cerebral malaria, a disease associated with high mortality and long-term neurological sequelae, remains poorly understood. In this study, we utilized the classical model of experimental cerebral malaria (*Plasmodium berghei* ANKA-infected C57BL/6 mice) to investigate the dynamics and response of resident brain cell populations, particularly microglia, and the influx of other leukocytes during the development of experimental cerebral malaria. By employing flow cytometry and established markers for different leukocyte populations, we were able to discern and document an increase in the number of Ly6C⁺ T cells (CD45^{hi}CD11b⁻CD3⁺ cells), inflammatory monocytes (CD45^{hi}CD11b⁺TMEM119⁻CD206⁻ cells), resident macrophages (CD45^{hi}CD11b⁺TMEM119⁻CD206⁺ cells), and microglia (CD45^{low}CD11b⁺ TMEM119⁺CD206⁻ cells) following infection. Moreover, our *ex vivo* analysis demonstrated an increment in the overall number of inflammatory monocytes, resident macrophages and microglia expressing inducible nitric oxide synthase (iNOS), in addition to those producing interleukin-1 β or TNF. These findings highlight the pronounced reactivity of microglia in experimental cerebral malaria and provide valuable information on cell dynamics and immune responses in the brain.

KEYWORDS

experimental cerebral malaria, macrophages, malaria, microglia, nitric oxide, IL-1 β , iNOS, TNF

1 Introduction

Despite advancements in the diagnosis and treatment of cerebral malaria (CM), this severe form of the disease continues to represent a significant public health challenge. CM is a complication associated mainly with infection by the protozoan parasite *Plasmodium falciparum* infection, affecting primarily children under five years of age and nonimmune individuals (1). The condition presents as an encephalopathy, which is characterized by seizures and coma (2). Despite treatment, the mortality rate for patients with this complication exceeds 20% (3, 4). However, even if an individual's CM episode is reversed, they may still experience neurological and cognitive sequelae that can persist for years (5).

The data derived from post-mortem studies in humans (6, 7) and the extrapolations based on studies employing experimental cerebral malaria (ECM) models (8, 9) indicate that CM results from a complex interplay of mechanisms that perpetuate a vicious cycle. The key mechanisms involved include the adhesion of infected red blood cells (iRBCs) to the endothelium of microvessels in the central nervous system (CNS) (6, 8) and the production of systemic and local inflammatory mediators (10). These mediators activate endothelial cells and increase the expression of adhesion molecules, thereby facilitating the recruitment of immune cells to the brain and exacerbating RBC adhesion (11, 12). This can result in microvascular obstruction, hypoxia, and disruption of the blood-brain barrier (BBB) (13, 14).

In addition to the migration of cells from the innate and adaptive immune systems to the brain, which coincides with the onset of neurological signs of ECM and has been documented in post-mortem analyses of CM patients (7, 15–17), the literature also explores the role of resident immune cells of the brain parenchyma, such as microglia, and their involvement in the course of brain disease (18, 19). Microglia are derived from embryonic yolk sac precursors that occupy the embryonic region of the CNS during the early stages of embryogenesis, preceding the formation of the BBB (20, 21). Following the embryonic period, during homeostasis, these cells are able to maintain their constant population through self-renewal, independently of the influx of blood monocytes (22). Microglia play a crucial role in numerous physiological processes, including neurogenesis (23), blood vessel development (24), and the maintenance of the BBB (25). Furthermore, these cells are under constant surveillance, detecting and responding to alterations in the microenvironment, and are essential for the removal of cellular debris and metabolic waste (26, 27).

Morphological alterations in microglia have been documented days prior to the emergence of ECM, indicating that these cells possess the capacity to perceive and promptly respond to changes in the host environment driven by infection (28). The transcriptomic analysis of microglia conducted by Capuccini et al. (29) indicates that in the brains of mice subjected to *P. berghei* ANKA-induced ECM, these cells respond to infection by initially activating cell cycle pathways. As ECM signs become apparent, there is an increase in the expression of genes associated with immune responses and chemokine production. Furthermore, an *in vitro* study has demonstrated that microglial interaction with *P. berghei* ANKA-

iRBCs results in the production of TNF and interferon gamma inducible protein 10 (IP10) (18). Additionally, the incubation of synthetic hemozoin with a microglia cell line has been demonstrated to induce the production of TNF, IL-6, IL-1 β , and nitric oxide (NO) (30).

The present study, conducted with the *P. berghei* ANKA-C57BL/6 murine ECM, aims to expand the knowledge base regarding the immune cells present and flowing into the brain parenchyma in a temporal kinetic that precedes the development of ECM and during its establishment. Our observations indicated a notable accumulation of T cells and inflammatory monocytes concomitant with the onset of ECM. Additionally, our findings revealed a significant increase in the number of microglia, inflammatory monocytes, and resident macrophages expressing iNOS and producing IL-1 β or TNF.

2 Materials and methods

2.1 Mice, parasite, and infection

Six-to-eight-week-old female C57BL/6 mice, weighing between 16 and 20g, were provided by the Institute of Science and Technology in Biomodels (ICTB) of the Oswaldo Cruz Foundation (Fiocruz). Mice were housed in a specific pathogen-free room at the Oswaldo Cruz Institute (IOC), with free access to food and water, kept on a 12/12-hour light/dark cycle and at a constant temperature. All animal experiments were conducted in accordance with the guidelines and regulations set forth by the Animal Welfare Committee of the IOC-Fiocruz and were approved by the Committee. The experiments were performed under license (L-029/2020).

Infections were performed using *P. berghei* ANKA parasite that express green fluorescent protein (GFP; MR4 number: MRA-865) (31). The experimental group was infected intraperitoneally with 1×10^6 iRBCs in a final volume of 100 μ l per animal, with the source of the iRBCs being fresh blood from an infected mouse.

2.2 Parasitemia and temperature

On days 4 and 6 after infection, parasitemia and rectal temperature of the mice in the experimental groups were evaluated. The uninfected mice (Control group) were evaluated in parallel. Parasitemia level was determined via flow cytometric analysis of a diluted blood sample, prepared in phosphate-buffered solution (PBS). The percentage of iRBCs (GFP⁺ cells) was calculated after acquiring data from 20,000 RBCs. A thermocouple probe (Oakton[®] Acorn TM; Oakton Instruments, IL, USA) was utilized for measuring rectal temperature.

2.3 Blood-brain barrier permeability assay

To evaluate the BBB permeability, mice were anesthetized intraperitoneally with a combination of ketamine (100mg/kg) and

xylazine (10mg/kg), using a final volume of 100 μ l per animal. Subsequently, 100 μ l of a 2% solution of Evans Blue dye (Sigma) in PBS was injected intravenously through the orbital sinus. After one hour of dye circulation, the mice were euthanized and perfused transcardiacally with 20 mL of cold PBS. The brains were collected, weighed, and incubated in 3 mL of Formamide (Sigma) for 48 hours at 37°C. The concentration of Evans Blue dye in the formamide solution was determined by measuring its absorbance at a wavelength of 620 nm using a spectrophotometer. Calculations were based on a standard curve with a range of 1285 to 1.25 μ g/mL. The amount of dye was divided by the weight of the animal brain to express the concentration of dye per gram of tissue.

2.4 Tissue processing

Following the administration of anesthesia, mice were euthanized by exsanguination followed by transcardiac perfusion with 20 mL of cold PBS. The brain of each animal was removed, weighed and mechanically dissociated using the plunger of a syringe and a 70 μ m cell strainer (Falcon) in 20 mL of PBS supplemented with 5% fetal bovine serum (FBS). The cell suspension was then centrifuged for 10 minutes at 500 g, after which the cells were resuspended in 5 mL of PBS containing 30% isotonic Percoll solution (Sigma) at room temperature. A new centrifugation was then carried out for 10 minutes at 700 g without break, at room temperature. The myelin layer was removed with a *Pasteur* pipette, and the cells in the *pellet* were washed three times with 10 mL of PBS containing 5% FBS.

2.5 Immunophenotyping

The cells obtained following the processing of brain tissue were incubated with the Live/Dead Fixable Violet Dead Cell Stain Kit (Invitrogen), in accordance with the manufacturer's instructions. Subsequently, an incubation step was performed with a pool of antibodies, including anti-FC γ R III/II (CD16/32) (2,4G2, BD Biosciences), Alexa Fluor 700 anti-mouse CD11b (M1/70, BD Biosciences), FITC anti-mouse CD45 (30F11, BD Biosciences), Texas-Red anti-mouse F4/80 (T45-2342, BD Biosciences), PE anti-mouse CD3 (145-2C11, Invitrogen), APC-Cy7 anti-mouse Ly6C (AL-21, BD Biosciences), PerCP-eFluor 710 anti-mouse TMEM119 (V3RT1G0sz, Invitrogen) and/or PeCy7 anti-mouse CD206 (MR6F3, Invitrogen) for 30 minutes at 4°C in the dark. After immunolabeling of the surface molecules, cells were fixed and permeabilized with the Fixation/Permeabilization Kit (BD Biosciences) and incubated for 40–45 minutes at room temperature with the following fluorochrome-conjugated antibodies for intracellular targets: APC-eFluor 780 anti-mouse NOS2 (CXNFT, Invitrogen), APC anti-mouse IL-1 β (NJTEN 3, Invitrogen) and PE anti-mouse TNF (MP6-XT22, BD Biosciences) diluted in perm/wash solution. Samples were acquired on a CytoFLEX S flow cytometer (Beckman Coulter) and the data was analyzed using the FlowJo Software (BD Biosciences).

2.6 Statistical analysis

All statistical analyses were performed using Prism 8 (GraphPad). Data are presented as means with standard error of the mean (mean \pm SEM). Survival rates were analyzed using the Long-Rank (Mantel-Cox) test. Comparisons between two groups were made by unpaired t-test assuming statistical significance as $p < 0.05$. Comparisons between more than two groups were made by one-way ANOVA with Tukey's multiple comparisons test. The criterion for determining a significant difference was set at $p < 0.05$.

3 Results

3.1 Assessment of disease progression in an experimental cerebral malaria model

To corroborate prior literature data on the susceptibility of C57BL/6 mice to the development of ECM, we inoculated the animals with 1×10^6 *P. berghei* ANKA-iRBCs and evaluated them at days 4 and 6 post-infection. The parasitemia of all infected C57BL/6 mice increased progressively (Figure 1A), accompanied by significant hypothermia (Figure 1B) and a breakdown of the BBB (Figure 1C) at day 6 post-infection, consistent with the development of ECM. In our experimental setting, infection of C57BL/6 mice with *P. berghei* ANKA resulted in 100% mortality between days 6 and 9 post-infection (Figure 1D).

3.2 Dynamics of cell populations in the brain during experimental cerebral malaria

To identify the leukocyte populations present in the cerebral environment during homeostasis and those that infiltrate during ECM development, flow cytometry analyses were conducted. The expression profile of the markers CD45 (expressed in various leukocytes) and CD11b (expressed in myeloid-lineage cells) enable the identification of three distinct cell populations within the brain tissue. These cell populations were designated as CD45^{hi}CD11b⁻ cells (region 1), CD45^{hi}CD11b⁺ cells (region 2), and CD45^{low}CD11b⁺ cells (region 3) (Figure 2A). In naive animals, a pronounced presence of CD45^{low}CD11b⁺ cells was observed, representing 15–25% of the cells. Additionally, CD45^{hi}CD11b⁺ cells (0.4–2%) and CD45^{hi}CD11b⁻ cells (0.5–2.5%) were present to a lesser extent (Figure 2A). Following infection with *P. berghei* ANKA, the numbers of these cell populations remained constant at day 4 post-infection (Figure 2B), a time point preceding the development of clinical signs of ECM (Figure 1B). However, at day 6 post-infection, a change in the dynamics of these cells occurred, characterized by a significant increase in the number of these three cell populations (Figure 2B).

The notable expansion of the CD45^{hi}CD11b⁻ cell population, representing 15 to 25% of brain cells by day 6 post-infection, prompted further investigation into additional markers for enhanced identification. To specifically characterize this subset, we

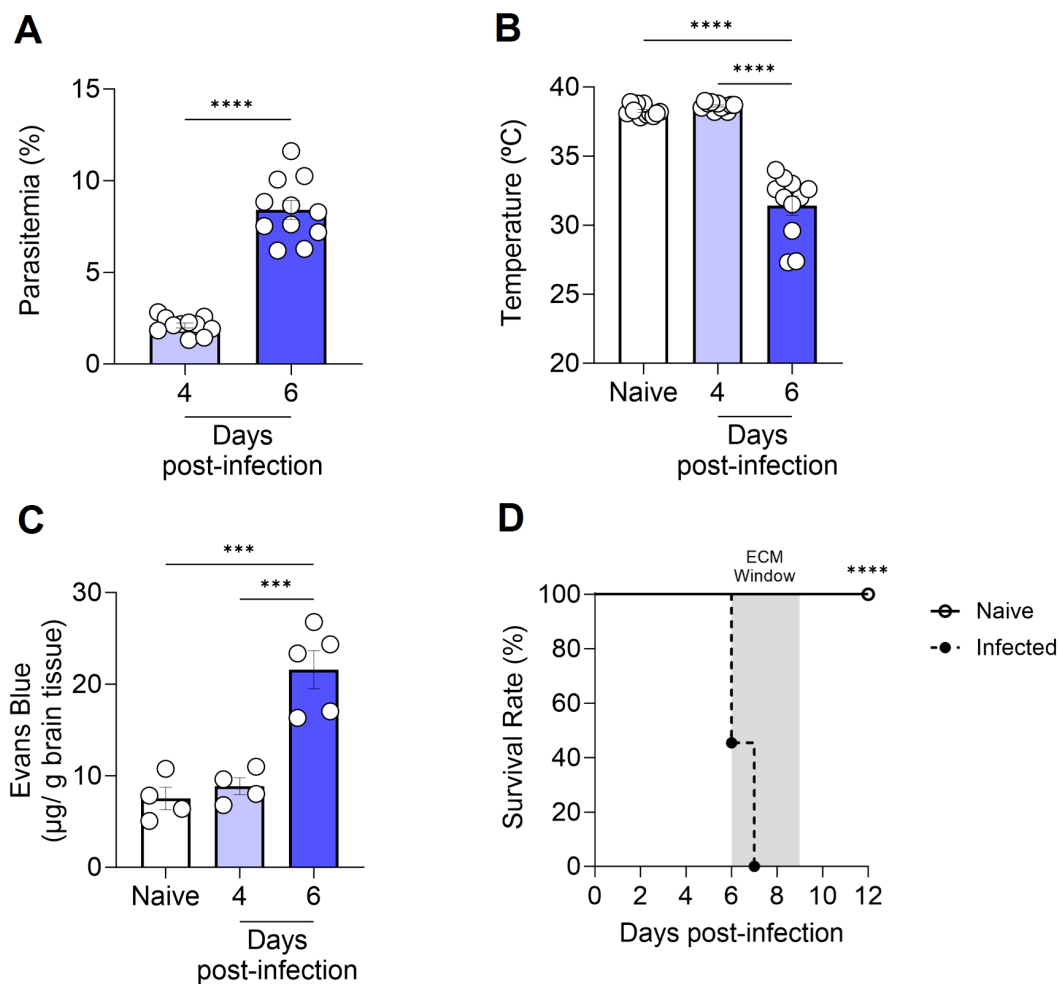


FIGURE 1

Progression of cerebral malaria in C57BL/6 mice infected with *Plasmodium berghei* ANKA. C57BL/6 mice were inoculated with 1×10^6 iRBCs. Parasitemia (percentage of GFP⁺ cells) (A), body temperature (B), extravasation of Evans Blue dye to the brain parenchyma (C), and survival rate (D) were assessed in naive and infected C57BL/6 mice at various time points. Significant differences between groups were analyzed using the following statistical tests: unpaired t-test (A), one-way ANOVA (B, C), and the Long-Rank test (D). The results were statistically significant at $p < 0.0006$ (***) and $p < 0.0001$ (****). Graphs A and B: 10 mice per group. Graph C: 4–5 mice per group. Graph D: 10–22 mice per group. The data were pooled from two independent experiments (A, B, D) or are representative of two independent experiments (C).

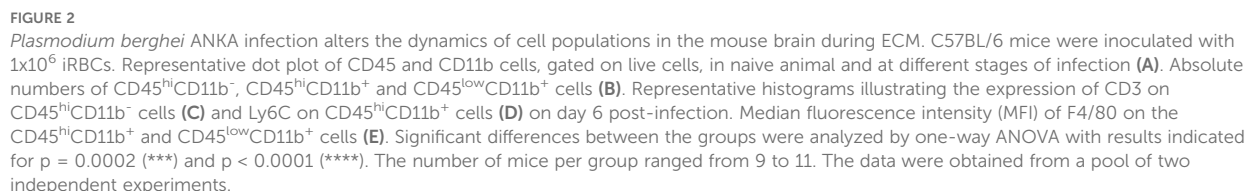
included CD3, a definitive T cell marker (Figure 2C, Supplementary Figure S2B), and Ly6C, also known as lymphocyte-6 antigen (Supplementary Figure S1) in our analysis. The Ly6C molecule is frequently expressed by specific subpopulations of T cells, monocytes and neutrophils (32, 33). A high proportion of the CD45^{hi}CD11b⁻ cells expressed both CD3 and Ly6C, indicating that this particular cell subset, which increases in the brain at day 6 post-infection is predominantly formed by Ly6C⁺ T cells.

On the other hand, a distinct Ly6C expression (Figure 2D) was evident in the CD45^{hi}CD11b⁺ cell population, while CD3 was not expressed (Supplementary Figure S1). Furthermore, our findings revealed that both CD45^{hi}CD11b⁺ and CD45^{low}CD11b⁺ cells are F4/80⁺ (a marker of cells of monocytic origin), as the majority of cells within these populations express this molecule (Supplementary Figure S1D). However, a notable distinction in expression levels was observed. In particular, the CD45^{hi}CD11b⁺ cell population

displayed a markedly elevated level of F4/80 molecule expression on their surface, in comparison to the CD45^{low}CD11b⁺ cell population (Figure 2E).

3.3 Phenotypic characterization of brain myeloid cell populations in homeostasis and experimental cerebral malaria

To provide a more comprehensive characterization of the myeloid cell populations (CD45^{hi}CD11b⁺ and CD45^{low}CD11b⁺ cells), we conducted an analysis utilizing the cellular markers TMEM119 and CD206. Previous studies have demonstrated that under homeostatic conditions, microglia exhibit elevated levels of TMEM119 expression (34) and low expression of CD206, a mannose receptor (35).



Therefore, based on our analyses and the findings of previous literature (36, 37), we identified (Supplementary Figure S2) and quantified the total number (Figures 4A–C) and percentage

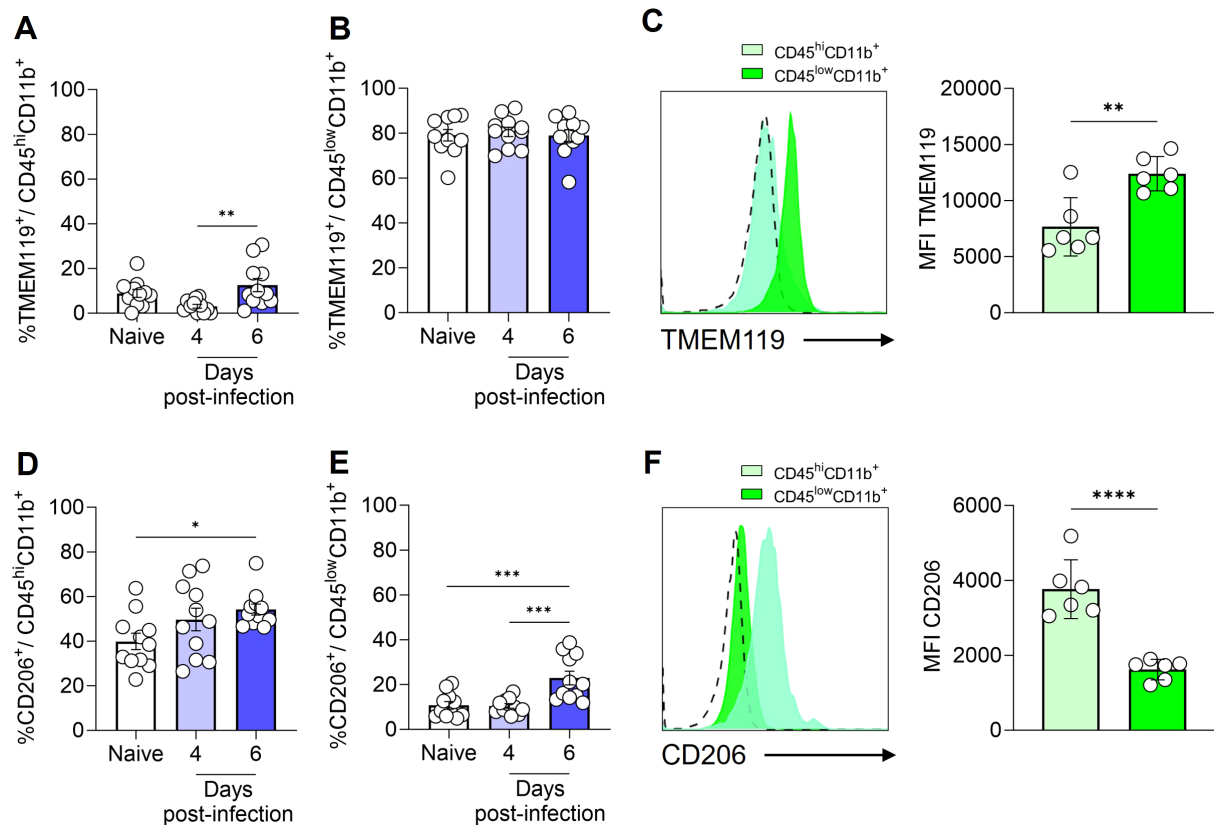


FIGURE 3

Expression of TMEM119 and CD206 by monocytes/macrophages and microglia. C57BL/6 mice were inoculated with 1×10^6 iRBCs. Percentage of TMEM119⁺ cells within CD45^{hi}CD11b⁺F4/80⁺ (A) and CD45^{low}CD11b⁺F4/80⁺ (B) populations. Representative histogram and bar plots showing the median fluorescence intensity (MFI) of TMEM119 on the CD45^{hi}CD11b⁺ and CD45^{low}CD11b⁺ cells (C). Percentage of CD206⁺ cells within CD45^{hi}CD11b⁺F4/80⁺ (D) and CD45^{low}CD11b⁺F4/80⁺ (E) populations. Representative histogram and bar plots showing the MFI of CD206 on the CD45^{hi}CD11b⁺ and CD45^{low}CD11b⁺ cells (F). The dashed line in the histograms represents the FMO (fluorescence minus one) control. Significant differences between groups were analyzed by one-way ANOVA, with the results indicated for $p = 0.03$ (*), $p = 0.007$ (**), $p = 0.0006$ (***) and $p < 0.0001$ (****). The number of mice per group ranged from 9 to 11. The data were obtained from two independent experiments.

(Figures 4D–F) of inflammatory monocytes (CD45^{hi}CD11b⁺TMEM119⁺CD206⁺), resident macrophages (CD45^{hi}CD11b⁺TMEM119⁺CD206⁺) and microglia (CD45^{low}CD11b⁺TMEM119⁺CD206⁺) in the brain of naive and infected animals. This refined characterization, based on the expression or not of CD206 and TMEM, indicates that by day 6 of ECM development in *P. berghei* ANKA-infected mice, the number of microglia rose from 2×10^3 to 6×10^3 cells, representing a dramatic 300% expansion (Figure 4C). Additionally, the number of inflammatory monocytes and resident macrophages in the brain exhibited a significant increase, from a minimal quantity to 1×10^3 cells (inflammatory monocytes; Figure 4A) and 2.7×10^3 cells (resident macrophages; Figure 4B). The percentage of inflammatory monocytes (Figure 4D) and resident macrophages (Figure 4E) followed a similar trend, corresponding to the observed changes in cell numbers. However, the percentage elevation of microglia (Figure 4F) was less pronounced, likely attributable to the concurrent increase in other cell types within the brain. These findings indicate that, at the onset of ECM, the brain experiences a robust inflammatory response.

3.4 IL-1 β , TNF and iNOS expression by inflammatory monocytes, resident macrophages and microglia

Next, we assessed the production of IL-1 β , TNF, and the expression of iNOS by inflammatory monocytes (CD45^{hi}CD11b⁺TMEM119⁺CD206⁺), resident macrophages (CD45^{hi}CD11b⁺TMEM119⁺CD206⁺), and microglia (CD45^{low}CD11b⁺TMEM119⁺CD206⁺) (Supplementary Figure S3). On day 6 post-infection, the increase in the total number of inflammatory monocytes, resident macrophages, and microglia, as previously described in Figures 4A–C, was accompanied by a rise in the number of cells from these same populations expressing iNOS (Figures 5A–C), and producing IL-1 β (Figures 5D–F) or TNF (Figures 5G–I).

It is important to note that while the total number of iNOS⁺, IL-1 β ⁺, and TNF⁺ inflammatory monocytes, resident macrophages and microglia increased over the course of infection, the percentage of iNOS⁺ cells among each population (inflammatory monocytes, macrophages and microglia) either remained constant or decreased

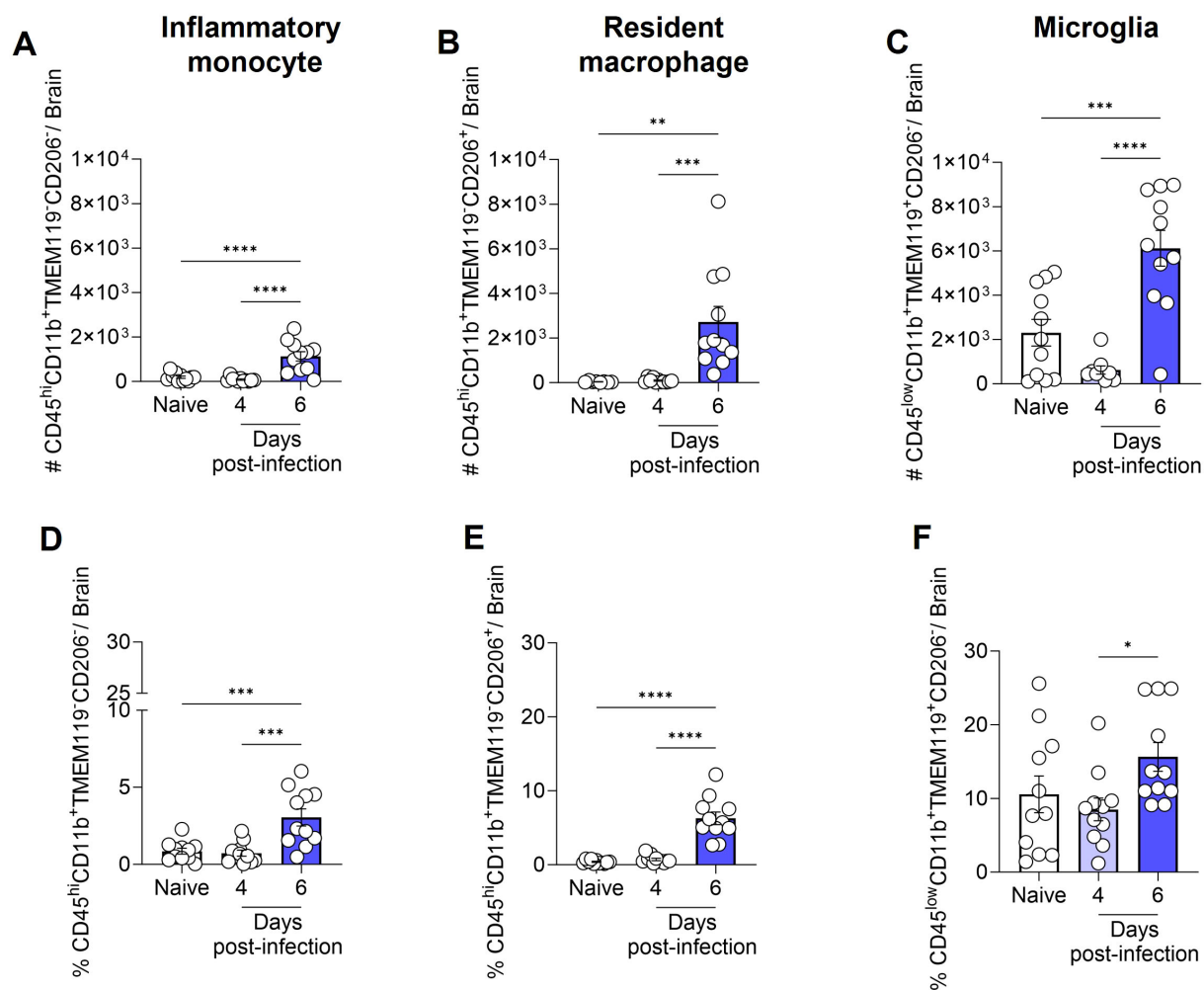


FIGURE 4

Total number and percentage of inflammatory monocytes, resident macrophages and microglia in the mouse brain following infection with *Plasmodium berghei* ANKA. C57BL/6 mice were inoculated with 1×10^6 iRBCs. The absolute number (A–C) and percentage (D–F) of inflammatory monocytes ($CD45^{hi}CD11b^{+}TMEM119^{+}CD206^{-}$), resident macrophages ($CD45^{hi}CD11b^{+}TMEM119^{-}CD206^{+}$), and microglia ($CD45^{low}CD11b^{+}TMEM119^{+}CD206^{-}$). Significant differences between groups were analyzed by one-way ANOVA, with results indicated for $p < 0.04$ (*), $p < 0.001$ (**), $p < 0.0005$ (***), and $p < 0.0001$ (****). The number of mice per group ranged from 8 to 11. The data were obtained from a pool of two independent experiments.

(Supplementary Figure S4A–C). Conversely, the percentage of $IL-1\beta^{+}$ and TNF^{+} microglia increased by day 6 post-infection (Supplementary Figure S4F, I). However, given the low number of inflammatory monocytes and resident macrophages in the brains of naive animals, which resulted in high variability in the percentage analysis, no significant difference was observed in the percentage of $IL-1\beta^{+}$ and TNF^{+} inflammatory monocytes and resident macrophages between naive and infected animals (Supplementary Figure S4D, E, G, H).

4 Discussion

The data presented herein provide knowledge of the dynamics of the inflammatory response of mononuclear cells in the CNS, including microglia and other populations associated with and

recruited to the brain during *P. berghei* ANKA infection of C57BL/6 mice, an experimental model of ECM.

The initial investigations into microglia activation during CM in humans (38) and in experimental models (28) were conducted in the late 1990s and revealed several important aspects, including local inflammation, which should be considered in the quest to understand the pathophysiological mechanisms of CM. In these studies, microglia activation was described through changes in their morphology and expression of MRP8 and MRP14, calcium-binding sensor proteins of activated monocytes. At that time, the identification of the cell of interest was achieved through the use of classical histology and immunohistochemistry, employing markers that are currently known to be inadequate for distinguishing microglia from other resident and recruited CNS mononuclear cells (28, 38).

Two additional studies from the mid-2000s employing distinct methodologies have corroborated the activation of microglia during

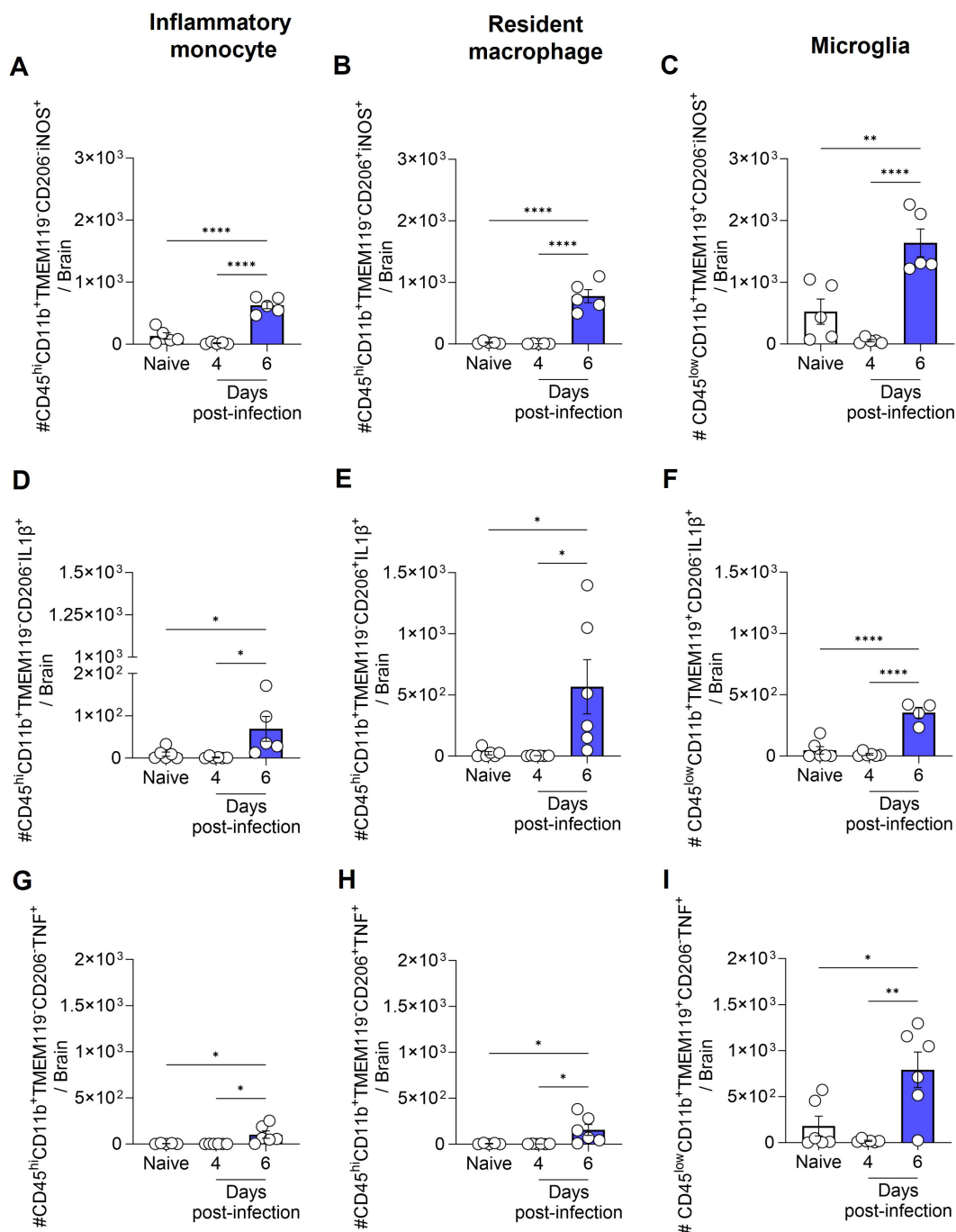


FIGURE 5

Total number of inflammatory monocytes, resident macrophages and microglia expressing iNOS, and producing IL-1 β or TNF during ECM. C57BL/6 mice were inoculated with 1×10^6 iRBCs. The absolute number of iNOS⁺ (A–C), IL-1 β ⁺ (D–F), and TNF⁺ (G–I) cells among inflammatory monocytes, resident macrophages and microglia. Significant differences between groups were analyzed by one-way ANOVA, with results indicated for $p < 0.03$ (*), $p < 0.002$ (**), and $p < 0.0001$ (****). The number of mice per group ranged from 4 to 6. Representative data from two independent experiments.

ECM. The initial study employed automated histological analysis, which considered Iba1 expression and morphological changes in its conclusions (39). The second study utilized transcriptomic analysis of microglia isolated from the brains of C57BL/6 mice infected with *P. berghei* ANKA. This analysis was conducted at two distinct time points, prior to and during the clinical manifestations of ECM. The

results demonstrated that genes are differentially expressed at these two time points following infection (29).

In the present study, a combination of distinct cell markers was employed to identify specific cell populations in the brains of C57BL/6 mice infected with *P. berghei* ANKA, utilizing flow cytometry. The differential expression of the CD45 and CD11b molecules enable the

identification of distinct cell populations. The observed differences in CD45 expression levels (CD45^{hi} and CD45^{low}) between myeloid cells (CD11b⁺) indicate the existence of two distinct myeloid cell populations. However, previous studies have indicated that CD45 expression can be altered during infections (40, 41), and thus we included additional markers to more accurately identify and characterize these cells. These included the transmembrane protein TMEM119 and the mannose receptor CD206.

Bennett et al. (42) demonstrated that TMEM119 is exclusively expressed by microglia during homeostasis in both humans and mice. This protein has been identified as a potential microglial marker that is capable of differentiating resident microglia from blood-derived macrophages in the brain (42). This finding has been corroborated by several subsequent studies (43–46). Furthermore, Hattori et al. (37) employed the molecule CD206 to distinguish microglia (CD206⁻ cells) from resident macrophages (CD206⁺ cells) (37), a strategy also employed in other studies (36, 47, 48).

The combination of the aforementioned markers with more traditional ones revealed that the majority of CD45^{low}CD11b⁺ cells were TMEM119⁺, and this population was identified as microglia. Conversely, CD45^{hi}CD11b⁺ cells were predominantly negative for TMEM119. A subset of these TMEM119⁻ cells were also CD206⁻, thus classifying them as inflammatory monocytes, while the remaining subset expressed CD206, resulting in their classification as resident macrophages. Following the precise characterization of these three mononuclear phagocyte populations, the findings indicate that C57BL/6 animals infected with *P. berghei* ANKA exhibit an influx of inflammatory monocytes from the periphery to the brain, detectable on day 6 post-infection. Furthermore, a notable increase in the overall number of resident macrophages and microglia was observed at this same time, indicating that all these cell types can sense and respond dynamically to the infectious process, potentially contributing to the local immune landscape during ECM progression. However, while the present study provides unequivocal evidence of the expansion of these CNS-resident and infiltrating phagocytes during ECM, it does not establish a causal link between these changes and disease pathogenesis. This is acknowledged as a limitation of the current study. Upcoming experimental approaches employing depletion or inhibition strategies (e.g., clodronate liposomes or genetic models) at the correct stage of disease will be essential to determine the functional contribution of these cell populations to ECM progression.

The observed increase in the number of microglia in the acute phase of ECM may be attributed to the proliferation of these cells. These findings are consistent with those previously reported by Capuccini et al. (29), who observed an increase in the expression of genes related to cell proliferation before the onset of ECM, as well as an increase in the number of these cells in the brain during ECM. At the onset of ECM clinical signals, the transcriptomic analysis also demonstrated an upregulation of genes involved in the immune response and chemokine production (29).

Data from our experimental model revealed that, in addition to inflammatory monocytes and resident macrophages, microglia also exhibited a significant increase in the total number of IL-1β⁺ and TNF⁺

cells at day 6 post-infection, thereby highlighting the activation of pro-inflammatory pathways within the CNS. The production of IL-1β and TNF in the brain during *Plasmodium* infection has important functional implications for the pathogenesis of both ECM and CM. In murine models, TNF is essential for endothelial activation, BBB breakdown, and neuroinflammation, largely through upregulation of ICAM-1/VCAM-1 and recruitment of leukocytes to brain microvessels (49–51). Although IL-1β is not required for ECM development (52), it may exacerbate vascular permeability and inflammatory signaling once inflammation is established (53). In human CM, elevated levels of TNF and IL-1β have been found in brain tissue and plasma, correlating with vascular damage, immune cell infiltration, and neuronal injury (54, 55). These cytokines likely contribute to both endothelial dysfunction and neuronal pathology in CM, reinforcing their relevance as potential targets for therapeutic intervention.

Interestingly, studies conducted in mice deficient in NLRP3, caspase-1, the adaptor protein ASC, or the IL-1 receptor demonstrated that these mice exhibited comparable disease outcomes to wild-type mice, indicating that the activation of the inflammasome pathway does not play a significant role in the immunopathology caused by *P. berghei* ANKA (52, 56). However, Strangward P. et al. (57) observed that IL-33 therapy, in conjunction with antimalarial drugs, selectively inhibited the NLRP3-IL-1β inflammasome axis in microglia and monocytes, resulting in a significant reduction in IL-1β production in both cell types (57). This, in turn, led to an improvement in the treatment success of established ECM (57). In addition, a recent study showed that mice with combined deficiencies of caspases-8/1/11 or caspase-8/gasdermin-D (GSDM-D) exhibited impaired capacity to produce both TNF and IL-1β, and demonstrated high resistance to the development of ECM (58).

Despite the observed increase in the absolute number and percentage of IL-1β- and TNF-producing microglia throughout the course of infection, as well as an increase in the absolute number of cells expressing iNOS, the inducible form of the nitric oxide (NO)-producing enzyme, the percentage of cells expressing iNOS was found to be reduced. NO plays a fundamental role in the functioning of the brain, regulating blood flow and maintaining vascular integrity (59, 60). Furthermore, NO prevents the excessive adhesion of leukocytes and platelet aggregation in cerebral microvasculature, thereby preventing blockages and inflammation (61–63).

Nevertheless, the role of NO in malaria remains a topic of debate (64). A number of studies have demonstrated that the production of NO by immune cells is of significant importance in regulating the blood-stage parasite (65, 66), although it may potentially contribute to the development of CM (67). In contrast, it appears that in African children with malaria, NO exerts a protective effect rather than contributing to pathology (68). This observation is further supported by *in vivo* experiments conducted on mice deficient in iNOS or eNOS, which indicated that the low bioavailability of NO is associated with the development of ECM. The iNOS^{-/-} or eNOS^{-/-} animals exhibited parasitemia and ECM development course comparable to that of the control group (69, 70), while administration of exogenous NO protected the animals from ECM (63, 70). Indeed, several mechanisms have

been described in malaria that result in a decrease in the bioavailability of NO (70, 71).

Curiously, our observation of the relative reduction (percentage) of iNOS expression in microglia throughout infection may be directly correlated with increased proliferation during ECM development. This hypothesis is consistent with the findings of Maksoud et al. (72), who describe that microglia exhibit basal iNOS activity and that the iNOS/NO signaling pathway inhibits microglial cell proliferation by activating protein kinase G (PKG) (72). However, this remains speculative and should be interpreted with caution. Validation of this potential mechanism will require experiments using proliferation markers, such as Ki-67.

Although not the primary focus of this study, we were able to observe a significant increase in the number of T cells (CD45^{hi}CD11b⁺CD3⁺) expressing the lymphocyte-6 antigen (Ly6C) on their surface in the brain during the acute phase of ECM, a potentially novel and intriguing finding. The migration and adhesion of CD8 T cells to the cerebral vascular endothelium and their association with pathology have been previously described in CM and ECM (7, 15, 73). It is of interest to note that this is the first report, to the best of our knowledge, in which T cells expressing Ly6C have been observed in the brain during ECM. Our current analysis, however, did not determine the specific T cell lineage of these Ly6C⁺ T cells, but it is plausible that they belong to the CD8 T cell subset. Prior studies have established a correlation between Ly6C expression by CD8 T cells and augmented activation, cytotoxic effector function, and cytokine production (74–76). In particular, Kusaka et al. demonstrated that Ly6C⁺ CD8 T cells constitute a major source of IFN- γ during *Legionella pneumophila* infection, thereby emphasizing their role in regulating the inflammatory response. Prospective studies employing additional markers such as CD8, combined with functional assays to evaluate cytokine secretion and cytotoxic activity, will be essential to determine whether this subset of Ly6C⁺ T cells contributes to immunopathology in ECM. Such analyses may provide key insights into the cellular mechanisms underlying neuroinflammation and vascular damage in ECM, and open the opportunity to explore this population in the context of human CM. In conclusion, our findings revealed a notable elevation in the number of distinct immune cells, indicating their reactivity to *P. berghei* ANKA infection, which may be associated with the pathogenesis of ECM. Furthermore, we underscore the activation of microglia through an increase in the total number of cells expressing iNOS and producing TNF or IL-1 β . Collectively, our results provide valuable insights into the potential role of microglial reactivity in contributing to neuroinflammation during ECM. Future studies should focus on analyzing intermediate time points, such as days 5 and 5.5 post-infection, and employ monocyte and microglia depletion strategies to delineate their specific roles in the pathogenesis of ECM.

Data availability statement

The raw data supporting the conclusions of this article will be made available by the authors, without undue reservation.

Ethics statement

The animal study was approved by Ethics committee of the Instituto Oswaldo Cruz (CEUA-IOC, Fiocruz, license number L-29/2020). The study was conducted in accordance with the local legislation and institutional requirements.

Author contributions

LF-A: Formal analysis, Investigation, Methodology, Writing – original draft, Writing – review & editing. UO-G: Investigation, Writing – review & editing. MR-F: Investigation, Writing – review & editing. MR-A: Investigation, Writing – review & editing. LC: Writing – review & editing. CD-R: Writing – review & editing. FR-G: Funding acquisition, Investigation, Resources, Writing – review & editing, Conceptualization, Supervision.

Funding

The author(s) declare that financial support was received for the research and/or publication of this article. This work was supported by Conselho Nacional de Desenvolvimento Científico e Tecnológico – CNPq (FLRG: Universal 431230/2016-1), Fundação Carlos Chagas Filho de Amparo à Pesquisa do Estado do Rio de Janeiro – Faperj (FR-G: E-26/211.323/2019 and 26/210.420/2022) and Fiocruz – INOVA (FR-G: 8121512557). LC, CD-R and FR-G are PQ-fellows of the CNPq (LC: 316462/2021-7; CD-R: 310445/2017-5; FR-G: 311128/2022-0). LC and CD-R are also Cientistas do Nosso Estado of the Faperj (LC: E-26/200.314/2022 and CD-R: E-26/202.921/2018). The Laboratório de Pesquisa em Malária is an Associate Laboratory of the Instituto Nacional de Ciência e Tecnologia em Neuroimunomodulação of the CNPq (INCT-NIM/CNPq) Project 465489/2014–1 and of the Rede de Neuroinflamação da Faperj (Redes/Faperj, Project 26010.002418/2019).

Acknowledgments

The authors thank the Multi-user Research Facility of Flow Cytometry – Multiparametric Analysis, Instituto Oswaldo Cruz, Fundação Oswaldo Cruz, Rio de Janeiro, Brazil. The authors thank DVM Mônica Nogueira and her team of the Animal Experimentation Center (IOC, Fiocruz) for caring for the animals and supporting the experiments. LF-A, UO-G, MR-F, and MR-A are grateful to the Postgraduate Program in Cellular and Molecular Biology of the Instituto Oswaldo Cruz (IOC), Fiocruz, for the academic support and to Faperj and to the Coordenação de Aperfeiçoamento de Pessoal de Nível Superior (CAPES) for MSc and doctoral fellowships.

Conflict of interest

The authors declare that the research was conducted in the absence of any commercial or financial relationships that could be construed as a potential conflict of interest.

Publisher's note

All claims expressed in this article are solely those of the authors and do not necessarily represent those of their affiliated

organizations, or those of the publisher, the editors and the reviewers. Any product that may be evaluated in this article, or claim that may be made by its manufacturer, is not guaranteed or endorsed by the publisher.

Supplementary material

The Supplementary Material for this article can be found online at: <https://www.frontiersin.org/articles/10.3389/fimmu.2025.1494418/full#supplementary-material>

References

- World Health Organization. World malaria report(2023). Available online at: <https://www.who.int/teams/global-malaria-programme/reports/world-malaria-report-2023> (Accessed September 9, 2024).
- World Health Organization. Severe falciparum malaria. *Trans R Soc Trop Med Hyg.* (2000) 94:1–90. doi: 10.1016/S0035-9203(00)90300-6
- Dondorp AM, Fanello CI, Hendriks IC, Gomes E, Seni A, Chhaganlal KD, et al. Artesunate versus quinine in the treatment of severe falciparum malaria in African children (AQUAMAT): an open-label, randomised trial. *Lancet.* (2010) 376:1647–57. doi: 10.1016/S0140-6736(10)61924-1
- Dondorp A, Nosten F, Stepniewska K, Day N, White N. Artesunate versus quinine for treatment of severe falciparum malaria: a randomised trial. *Lancet.* (2005) 366:717–25. doi: 10.1016/S0140-6736(05)67176-0
- Rosa-Goncalves P, Ribeiro-Gomes FL, Daniel-Ribeiro CT. Malaria related neurocognitive deficits and behavioral alterations. *Front Cell Infect Microbiol.* (2022) 12:829413. doi: 10.3389/fcimb.2022.829413
- Taylor TE, Fu WJ, Carr RA, Whitten RO, Mueller JG, Fosiko NG, et al. Differentiating the pathologies of cerebral malaria by postmortem parasite counts. *Nat Med.* (2004) 10:143–5. doi: 10.1038/nm986
- Riggle BA, Mangani M, Maric D, Johnson KR, Lee MH, Abath Neto OL, et al. CD8+ T cells target cerebrovasculature in children with cerebral malaria. *J Clin Invest.* (2020) 130:1128–38. doi: 10.1172/JCI133474
- Baptista FG, Pamplona A, Pena AC, Mota MM, Pied S, Vigário AM. Accumulation of Plasmodium berghei-infected red blood cells in the brain is crucial for the development of cerebral malaria in mice. *Infect Immun.* (2010) 78:4033–9. doi: 10.1128/IAI.00079-10
- Swanson PA, Hart GT, Russo MV, Nayak D, Yazew T, Peña M, et al. CD8+T Cells Induce Fatal Brainstem Pathology during Cerebral Malaria via Luminal Antigen-Specific Engagement of Brain Vasculature. *PLoS Pathog.* (2016) 12:1–34. doi: 10.1371/journal.ppat.1006022
- Dunst J, Kamena F, Matuschewski K. Cytokines and chemokines in cerebral malaria pathogenesis. *Front Cell Infect Microbiol.* (2017) 7:324. doi: 10.3389/fcimb.2017.00324
- Bauer PR, van der Heyde HC, Sun G, Specian RD, Granger DN. Regulation of endothelial cell adhesion molecule expression in an experimental model of Cerebral Malaria. *Microcirculation.* (2002) 9(6):463–70. doi: 10.1038/sj.mn.7800159
- Howland SW, Poh CM, Rénia L. Activated brain endothelial cells cross-present malaria antigen. *PLoS Pathog.* (2015) 11:1–24. doi: 10.1371/journal.ppat.1004963
- Penet MF, Viola A, Confort-Gouny S, Le Fur Y, Duhamel G, Kober F, et al. Imaging experimental cerebral malaria *in vivo*: Significant role of ischemic brain edema. *J Neurosci.* (2005) 25:7352–8. doi: 10.1523/JNEUROSCI.1002-05.2005
- Moreira AS, Estado V, Malvar DC, Sanches GS, Gomes F, Tibirica E, et al. L-arginine supplementation and thromboxane synthase inhibition increases cerebral blood flow in experimental cerebral malaria. *Sci Rep.* (2019) 9:1–13. doi: 10.1038/s41598-019-49855-x
- Belnoue E, Kayibanda M, Vigario AM, Deschemin J, Rooijen NV, Viguier M, et al. On the pathogenic role of thromboxane synthase inhibition increases cerebral malaria. *J Immunol.* (2002) 169:6369–75. doi: 10.4049/jimmunol.169.11.6369
- Hansen DS, Bernard NJ, Nie CQ, Schofield L. NK Cells Stimulate Recruitment of CXCR3+ T Cells to the Brain during Plasmodium berghei - Mediated Cerebral Malaria. *J Immunol.* (2007) 178:5779–88. doi: 10.4049/jimmunol.178.9.5779
- Dorovini-Zis K, Schmidt K, Huynh H, Fu W, Whitten RO, Milner D, et al. The neuropathology of fatal cerebral malaria in Malawian children. *Am J Pathol.* (2011) 178:2146–58. doi: 10.1016/j.ajpath.2011.01.016
- Shrivastava SK, Dalko E, Delcroix-Genete D, Herbert F, Cazenave PA, Pied S. Uptake of Parasite-derived vesicles by astrocytes and microglial phagocytosis of infected erythrocytes may drive neuroinflammation in cerebral malaria. *Glia.* (2017) 65:75–92. doi: 10.1002/glia.23075
- Ginhoux F, Greter M, Leboeuf M, Nandi S, See P, Gokhan S, et al. Fate mapping analysis reveals that adult microglia derive from primitive macrophages. *Science* (80-). (2010) 330:841–5. doi: 10.1126/science.1194637
- Swinnen N, Smolders S, Avila A, Notelaers K, Paesen R, Ameloot M, et al. Complex invasion pattern of the cerebral cortex by microglial cells during development of the mouse embryo. *Glia.* (2013) 61:150–63. doi: 10.1002/glia.22421
- Ajami B, Bennett JL, Krieger C, Tetzlaff W, Rossi FMV. Local self-renewal can sustain CNS microglia maintenance and function throughout adult life. *Nat Neurosci.* (2007) 10:1538–43. doi: 10.1038/nn2014
- Paolicelli RC, Bolasco G, Pagani F, Maggi L, Scianni M, Panzanelli P, et al. Synaptic pruning by microglia is necessary for normal brain development. *Science* (80-). (2011) 333:1456–8. doi: 10.1126/science.1202529
- Dudiki T, Meller J, Mahajan G, Liu H, Zhevhlakova I, Stefl S, et al. Microglia control vascular architecture via a TGFβ1 dependent paracrine mechanism linked to tissue mechanics. *Nat Commun.* (2020) 11(1):986. doi: 10.1038/s41467-020-14787-y
- Haruwaka K, Ikegami A, Tachibana Y, Ohno N, Konishi H, Hashimoto A, et al. Dual microglia effects on blood brain barrier permeability induced by systemic inflammation. *Nat Commun.* (2019) 10:1–17. doi: 10.1038/s41467-019-13812-z
- Davalos D, Grutzendler J, Yang G, Kim JV, Zuo Y, Jung S, et al. ATP mediates rapid microglial response to local brain injury *in vivo*. *Nat Neurosci.* (2005) 8:752–8. doi: 10.1038/nn1472
- Nimmerjahn A, Kirchhoff F, Helmchen F. Resting microglial cells are highly dynamic surveillants of brain parenchyma *in vivo*. *Science* (80-). (2005) 308:1314–8. doi: 10.1126/science.1110647
- Medana IM, Hunt NH, Chan-Ling T. Early activation of microglia in the pathogenesis of fatal murine cerebral malaria. *Glia.* (1997) 19:91–103. doi: 10.1002/(SICI)1098-1136(199702)19:2<91::AID-GLIA1>3.0.CO;2-C
- Capuccini B, Lin J, Talavera-López C, Khan SM, Sodenkamp J, Spaccapelo R, et al. Transcriptomic profiling of microglia reveals signatures of cell activation and immune response, during experimental cerebral malaria. *Sci Rep.* (2016) 6:1–11. doi: 10.1038/srep39258
- Velagapudi R, Kosoko AM, Olajide OA. Induction of neuroinflammation and neurotoxicity by synthetic hemozoin. *Cell Mol Neurobiol.* (2019) 39:1187–200. doi: 10.1007/s10571-019-00713-4
- Franke-Fayard B, Trueman H, Ramesar J, Mendoza J, van der Keur M, van der Linden R, et al. A Plasmodium berghei reference line that constitutively expresses GFP at a high level throughout the complete life cycle. *Mol Biochem Parasitol.* (2004) 137:23–33. doi: 10.1016/j.molbiopara.2004.04.007
- Peters NC, Pagán AJ, Lawyer PG, Hand TW, Henrique Roma E, Stamper LW, et al. Chronic parasitic infection maintains high frequencies of short-lived Ly6C+CD4+ Effector T cells that are required for protection against re-infection. *PLoS Pathog.* (2014) 10(12):e1004538. doi: 10.1371/journal.ppat.1004538
- Jergović M, Coplen CP, Uhrhau JL, Besselsen DG, Cheng S, Smithey MJ, et al. Infection-induced type I interferons critically modulate the homeostasis and function of CD8+ naïve T cells. *Nat Commun.* (2021) 12:1–16. doi: 10.1038/s41467-021-25645-w

34. Ruan C, Elyaman W. A new understanding of TMEM119 as a marker of microglia. *Front Cell Neurosci.* (2022) 16:902372. doi: 10.3389/fncel.2022.902372
35. Böttcher C, Schlickeiser S, Sneebroeck MAM, Kunkel D, Knop A, Paza E, et al. Human microglia regional heterogeneity and phenotypes determined by multiplexed single-cell mass cytometry. *Nat Neurosci.* (2019) 22:78–90. doi: 10.1038/s41593-018-0290-2
36. Li Q, Barres BA. Microglia and macrophages in brain homeostasis and disease. *Nat Rev Immunol.* (2018) 18:225–42. doi: 10.1038/nri.2017.125
37. Hattori Y, Kato D, Murayama F, Koike S, Asai H, Yamasaki A, et al. CD206+ macrophages transventricularly infiltrate the early embryonic cerebral wall to differentiate into microglia. *Cell Rep.* (2023) 42:112092. doi: 10.1016/j.celrep.2023.112092
38. Schluesener HJ, Kreamsner PG, Meyermann R. Widespread expression of MRP8 and MRP14 in human cerebral malaria by microglial cells. *Acta Neuropathol.* (1998) 96:575–80. doi: 10.1007/s004010050938
39. Hoffmann A, Pfeil J, Alfonso J, Kurz FT, Sahm F, Heiland S, et al. Experimental cerebral malaria spreads along the rostral migratory stream. *PLoS Pathog.* (2016) 12:1–24. doi: 10.1371/journal.ppat.1005470
40. Hermiston ML, Xu Z, Weiss A. CD45: A critical regulator of signaling thresholds in immune cells. *Annu Rev Immunol.* (2003) 21:107–37. doi: 10.1146/annurev.immunol.21.120601.140946
41. Honarpisheh P, Lee J, Banerjee A, Blasco-Conesa MP, Honarpisheh P, d'Aigle J, et al. Potential caveats of putative microglia-specific markers for assessment of age-related cerebrovascular neuroinflammation. *J Neuroinflamm.* (2020) 17:1–14. doi: 10.1186/s12974-020-02019-5
42. Bennett ML, Bennett FC, Liddelow SA, Ajami B, Zamanian JL, Fernhoff NB, et al. New tools for studying microglia in the mouse and human CNS. *Proc Natl Acad Sci.* (2016) 113:E1738–46. doi: 10.1073/pnas.1525528113
43. Duarte-Campos JF, Vázquez-Moreno CN, Martínez-Marcial M, Chavarría A, Ramírez-Carreto RJ, Velasco Velázquez MA, et al. Changes in neuroinflammatory markers and microglial density in the hippocampus and prefrontal cortex of the C58/J mouse model of autism. *Eur J Neurosci.* (2024) 59:154–73. doi: 10.1111/ejn.16204
44. Ma W, Oswald J, Rios Angulo A, Chen Q. Tmem119 expression is downregulated in a subset of brain metastasis-associated microglia. *BMC Neurosci.* (2024) 25:1–11. doi: 10.1186/s12868-024-00846-3
45. Nirwane A, Yao Y. SMAlow/undetectable pericytes differentiate into microglia and macrophage-like cells in ischemic brain. *Cell Mol Life Sci.* (2022) 79:1–14. doi: 10.1007/s00018-022-04322-1
46. Swanson MEV, Scotter EL, Smyth LCD, Murray HC, Ryan B, Turner C, et al. Identification of a dysfunctional microglial population in human Alzheimer's disease cortex using novel single-cell histology image analysis. *Acta Neuropathol Commun.* (2020) 8:1–16. doi: 10.1186/s40478-020-01047-9
47. Jurga AM, Paleczna M, Kuter KZ. Overview of general and discriminating markers of differential microglial phenotypes. *Front Cell Neurosci.* (2020) 14:198. doi: 10.3389/fncel.2020.00198
48. Van Hove H, Martens L, Scheyltjens I, De Vlaminck K, Pombo Antunes AR, De Prijck S, et al. A single-cell atlas of mouse brain macrophages reveals unique transcriptional identities shaped by ontogeny and tissue environment. *Nat Neurosci.* (2019) 22:1021–35. doi: 10.1038/s41593-019-0393-4
49. Rudin W, Eugster HP, Bordmann G, Bonato J, Müller M, Yamage M, et al. Resistance to cerebral malaria in tumor necrosis factor- α /beta-deficient mice is associated with a reduction of intercellular adhesion molecule-1 up-regulation and T helper type 1 response. *Am J Pathol.* (1997) 150:257–66.
50. Piguet PF, Da Kan C, Vesin C. Role of the tumor necrosis factor receptor 2 (TNFR2) in cerebral malaria in mice. *Lab Invest.* (2002) 82:1155–66. doi: 10.1097/01.LAB.0000028822.94883.8A
51. Nishioku T, Matsumoto J, Dohgu S, Sumi N, Miyao K, Takata F, et al. Tumor necrosis factor- α mediates the blood-brain barrier dysfunction induced by activated microglia in mouse brain microvascular endothelial cells. *J Pharmacol Sci.* (2010) 112:251–4. doi: 10.1254/jphs.09292SC
52. Kordes M, Matuschewski K, Hafalla JCR. Caspase-1 activation of interleukin-1 β (IL-1 β) and IL-18 is dispensable for induction of experimental cerebral malaria. *Infect Immun.* (2011) 79:3633–41. doi: 10.1128/IAI.05459-11
53. Rénia L, Howland SW, Claser C, Gruner AC, Suwanarusk R, Teo TH, et al. Cerebral malaria mysteries at the blood-brain barrier. *Virulence.* (2012) 3:193–201. doi: 10.4161/viru.19013
54. Brown H, Turner G, Rogerson S, Tembo M, Mwenechanya J, Molyneux M, et al. Cytokine expression in the brain in human cerebral malaria. *J Infect Dis.* (1999) 180:1742–6. doi: 10.1086/315078
55. Idro R, Marsh K, John CC, Newton CRJ. Cerebral Malaria: mechanisms of brain injury and strategies for improved neurocognitive outcome. *Pediatr Res.* (2010) 68:267–74. doi: 10.1080/10610278.2013.844812
56. Reimer T, Shaw MH, Franchi L, Coban C, Ishii KJ, Akira S, et al. Experimental cerebral malaria progresses independently of the Nlrp3 inflammasome. *Eur J Immunol.* (2010) 40:764–9. doi: 10.1002/eji.200939996
57. Strangward P, Haley MJ, Albornoz MG, Barrington J, Shaw T, Dookie R, et al. Targeting the IL33–NLRP3 axis improves therapy for experimental cerebral malaria. *Proc Natl Acad Sci U.S.A.* (2018) 115:7404–9. doi: 10.1073/pnas.1801737115
58. Pereira LMN, Assis PA, de Araújo NM, Durso DF, Junqueira C, Ataíde MA, et al. Caspase-8 mediates inflammation and disease in rodent malaria. *Nat Commun.* (2020) 11(1):4596. doi: 10.1038/s41467-020-18295-x
59. Forstermann U, Sessa WC. Nitric oxide synthases: regulation and function. *Eur Heart J.* (2012) 33:829–37. doi: 10.1093/eurheartj/ehr304
60. Bogdan C. Nitric oxide synthase in innate and adaptive immunity: An update. *Trends Immunol.* (2015) 36:161–78. doi: 10.1016/j.it.2015.01.003
61. Kubes P, Suzuki M, Granger DN. Nitric oxide: an endogenous modulator of leukocyte adhesion. *Proc Natl Acad Sci.* (1991) 88:4651–5. doi: 10.1073/pnas.88.11.4651
62. De Caterina R, Libby P, Peng HB, Thannickal VJ, Rajavashisth TB, Gimbrone MA, et al. Nitric oxide decreases cytokine-induced endothelial activation. Nitric oxide selectively reduces endothelial expression of adhesion molecules and proinflammatory cytokines. *J Clin Invest.* (1995) 96:60–8. doi: 10.1172/JCI118074
63. Zanini GM, Cabrales P, Barkho W, Frangos JA, Carvalho LJM. Exogenous nitric oxide decreases brain vascular inflammation, leakage and venular resistance during Plasmodium berghei ANKA infection in mice. *J Neuroinflamm.* (2011) 8:66. doi: 10.1186/1742-2094-8-66
64. Percário S, Moreira DR, Gomes BAQ, Ferreira MES, Gonçalves ACM, Laurindo PSOC, et al. Oxidative stress in malaria. *Int J Mol Sci.* (2012) 13:16346–72. doi: 10.3390/ijms131216346
65. Taylor-Robinson AW, Phillips RS, Severn A, Moncada S, Liew FY. The role of TH1 and TH2 cells in a rodent malaria infection. *Science* (80-). (1993) 260:1931–4. doi: 10.1126/science.8100366
66. Stevenson MM, Tam MF, Wolf SF, Sher A. IL-12-induced protection against blood-stage Plasmodium chabaudi AS requires IFN- γ and TNF- α and occurs via a nitric oxide-dependent mechanism. *J Immunol.* (1995) 155:2545–56. doi: 10.4049/jimmunol.155.5.2545
67. Maneerat Y, Viriyavejakul P, Punpoowong B, Jones M, Wilairatana P, Pongponratn E, et al. Inducible nitric oxide synthase expression is increased in the brain in fatal cerebral malaria. *Histopathology.* (2000) 37:269–77. doi: 10.1046/j.1365-2559.2000.00989.x
68. Anstey NM, Weinberg JB, Hassanali MY, Mwaikambo ED, Manyenga D, Misukonis MA, et al. Nitric oxide in Tanzanian children with malaria: inverse relationship between malaria severity and nitric oxide production/nitric oxide synthase type 2 expression. *J Exp Med.* (1996) 184:557–67. doi: 10.1084/jem.184.2.557
69. Favre N, Ryffel B, Rudin W. The development of murine cerebral malaria does not require nitric oxide production. *Parasitology.* (1999) 118:135–8. doi: 10.1017/S0031182098003606
70. Gramaglia I, Sobolewski P, Meays D, Contreras R, Nolan JP, Frangos JA, et al. Low nitric oxide bioavailability contributes to the genesis of experimental cerebral malaria. *Nat Med.* (2006) 12:1417–22. doi: 10.1038/nm1499
71. Ong PK, Melchior B, Martins YC, Hofer A, Orjuela-Sánchez P, Cabrales P, et al. Nitric oxide synthase dysfunction contributes to impaired cerebroarteriolar reactivity in experimental cerebral malaria. *PLoS Pathog.* (2013) 9(6):e1003444. doi: 10.1371/journal.ppat.1003444
72. Maksoud MJE, Tellios V, Xiang YY, Lu WY. Nitric oxide signaling inhibits microglia proliferation by activation of protein kinase-G. *Nitric Oxide - Biol Chem.* (2020) 94:125–34. doi: 10.1016/j.niox.2019.11.005
73. Hermesen C, Van De Wiel T, Mommers E, Sauerwein R, Eling W. Depletion of CD4+ or CD8+ T-cells prevents Plasmodium berghei induced cerebral malaria in end-stage disease. *Parasitology.* (1997) 114:7–12. doi: 10.1017/S0031182096008293
74. DeLong JH, Hall AO, Konradt C, Coppock GM, Park J, Harms Pritchard G, et al. Cytokine- and TCR-mediated regulation of T cell expression of Ly6C and Sca-1. *J Immunol.* (2018) 200:1761–70. doi: 10.4049/jimmunol.1701154
75. Kusaka Y, Kajiwara C, Shimada S, Ishii Y, Miyazaki Y, Inase N, et al. Potential Role of Gr-1 + CD8 + T Lymphocytes as a Source of Interferon- γ and M1/M2 Polarization during the Acute Phase of Murine Legionella pneumophila Pneumonia. *J Innate Immun.* (2018) 10:328–38. doi: 10.1159/000490585
76. Cornejo MG, Kharas MG, Werneck MB, Le Bras SV, Moore SA, Ball B, et al. Constitutive JAK3 activation induces lymphoproliferative syndromes in murine bone marrow transplantation models. *Blood.* (2009) 113:2746–54. doi: 10.1182/blood-2008-06